

Article

Effect of Ultrasonic Impact Strengthening on Surface Properties of 316L Stainless Steel Prepared by Laser Selective Melting

Hansong Chen ¹, Zhengye Zhang ¹, Jianmin Zhang ¹, Haibin Ji ², Zhao Meng ¹, Han Zhang ¹ and Xiankai Meng ^{1,*}

¹ School of Mechanical Engineering, Jiangsu University, Zhenjiang 212013, China

² School of Mechanical and Electrical Engineering, Xuzhou College of Industrial Technology, Xuzhou 221140, China

* Correspondence: xkmeng@ujs.edu.cn

Abstract: In order to study the effect of ultrasonic impact (UIP) on the microstructure and properties of 316L stainless steel prepared by selective laser melting (SLM), the hardness of the surface layer and depth direction of the sample were tested with a micro hardness tester. Finally, the friction and wear test of the sample was assessed using a friction and wear tester. The electrochemical corrosion test was carried out on the samples before and after the ultrasonic shock using a CHI660E electrochemical workstation. The results show that after the ultrasonic impact on the 316L stainless steel prepared by SLM, the surface produces plastic deformation and work hardening, which improves the hardness of the material surface and enhances the wear resistance of the sample surface. With ultrasound shocks affecting the near surface of the sample, a deformation layer of about 100 μm depth is formed. After the ultrasonic shock treatment, the self-corrosion potential of the sample in the 3.5% NaCl solution is slightly higher than the unproofed sample, and the density of the self-corrosion current is also lower than the unproofed sample, indicating that ultrasonic shock can reduce the corrosion rate of the material surface and enhance the abrasion resistance of the sample surface.

Keywords: 316L stainless steel; selective laser melting; ultrasonic impact; corrosion resistance; friction and wear performance



Citation: Chen, H.; Zhang, Z.; Zhang, J.; Ji, H.; Meng, Z.; Zhang, H.; Meng, X. Effect of Ultrasonic Impact Strengthening on Surface Properties of 316L Stainless Steel Prepared by Laser Selective Melting. *Coatings* **2022**, *12*, 1243. <https://doi.org/10.3390/coatings12091243>

Academic Editor: Paolo Castaldo

Received: 15 July 2022

Accepted: 17 August 2022

Published: 25 August 2022

Publisher's Note: MDPI stays neutral with regard to jurisdictional claims in published maps and institutional affiliations.



Copyright: © 2022 by the authors. Licensee MDPI, Basel, Switzerland. This article is an open access article distributed under the terms and conditions of the Creative Commons Attribution (CC BY) license (<https://creativecommons.org/licenses/by/4.0/>).

1. Introduction

Selective laser melting (SLM) is an additive manufacturing technology that enables high-performance and precision manufacturing of metal parts with complex structures, and thus has received extensive attention [1]. Compared with the traditional manufacturing process, selective laser melting (SLM) adopts point-by-point, line-by-line, and layer-by-layer forming methods, which can produce small batches with short production cycle, good flexibility, high precision, complex shapes, and high processing flexibility [2]. Zhang et al. [3] studied the effects of different process parameters on the microstructure, mechanical properties, wear characteristics, and corrosion behavior of SLM-formed NiTi. The results showed that high power and high scanning speed are beneficial to the formation of B2NiTi phase, while low power and low scanning speed are favorable for the formation of B19'NiTi phase. The samples formed with high power and high scanning speed have better abrasion resistance and corrosion resistance. Xu et al. [4] used SLM to reduce the metallurgical defects of Al-Cu-Mg alloy and improved the microstructure and hardness of this alloy. The obtained results showed that the microstructure consists of fine equiaxed crystals and columnar dendrites with pronounced pore and crack defects.

At present, the demand for ocean engineering equipment is increasing day by day, especially for some key components with high surface performance [5], among which pump components are widely used in marine equipment and ships, and the service life of pump components plays a key role in the performance of the whole system. 316L stainless steel

has excellent corrosion resistance [6], which is due to the passivation system of stainless steel itself, which can produce passivation film to resist Cl^- corrosion in seawater during the corrosion process. 316L stainless steel is widely used in the production of pump parts for marine equipment, ship blades, and oil pipelines. Due to the long-term service of pump parts in the marine environment, the working state is rapid rotation, and it is extremely prone to corrosion damage, cavitation and other behaviors [7].

Currently the corrosion of pump components in seawater is mainly divided into seawater corrosion, galvanic corrosion and chink corrosion [8]. The damage mainly occurs on the surface of the materials. Therefore, surface treatment technologies, such as chemical surface heat treatment [9], laser shock peening [10], surface shot peening [11], and ultrasonic impact technology [12], and other surface treatment technologies are adopted to improve the surface properties of the materials. Ultrasonic impact technology uses the impact needle of ultrasonic impact equipment to impact the surface of the material at high frequency to generate ultrasonic shock wave, thereby producing plastic deformation on the surface of the material, leading to the refinement of the internal microstructure and the introduction of effective residual stress, thus improving the hardness, wear resistance, and corrosion resistance of the surface of the material [10–15]. Compared with other surface treatment technologies, ultrasonic impact technology has the advantages of larger residual stress, better process controllability, more uniform machined surface, simple equipment, and low maintenance cost. Li et al. [16] conducted a micro-nano indentation test on the surface of SUS301 stainless steel by ultrasonic impact treatment. The study showed that under the same vibration frequency and different processing speeds, the size of micro-nano indentation was different, which supported surface hardening and achieved excellent wear resistance. Zhang et al. [17] studied the influence of ultrasonic shot peening (USP) on the microstructure evolution and corrosion resistance of Ti6Al4V manufactured by selective laser melting. The study showed that USP treatment generated compressive residual stress and significantly increased micro-hardness. The USP treatment could effectively improve the corrosion resistance of Ti6Al4V alloy manufactured by SLM. Alharbidi et al. [18] studied the effect of ultrasonic shot peening on the surface integrity of 316L stainless steel formed by SLM. After ultrasonic peening, the surface roughness of 316L stainless steel was decreased by about 176% and the micro-hardness was increased by about 90%. Eremin et al. [19] studied the influence of ultrasonic shock on the fatigue crack growth of Ti6Al4V prepared by SLM. The results showed that the fatigue durability of Ti6Al4V prepared by SLM after ultrasonic shock was about 60% higher. Yang et al. [20] carried out the forming test of 316L stainless steel by ultrasonic shock assisted melting electrode arc additive manufacturing. The results showed that the microstructure of formed parts was refined, and the micro-hardness and tensile properties were effectively improved after the introduction of ultrasonic shock. Yuan et al. [21] studied the grain refinement of TC4 titanium alloy by ultrasound-assisted laser fusion additive manufacturing. The experimental results showed that the microstructure of titanium alloy changed from typical coarse columnar crystals to fine columnar crystals, and ultrasonic impact effectively inhibited the epitaxial growth trend of β crystals and weakened the texture strength of β crystals.

In this paper, selective laser melting technology is used to manufacture 316L stainless steel samples. Microstructure, micro-hardness, friction and wear, electrochemical corrosion, and other tests were carried out on the untreated and ultrasonic shock 316L stainless steel samples manufactured by SLM to study the impact of ultrasonic shock on the surface properties of 316L stainless steel prepared by SLM.

2. Materials and Methods

The raw material selected for the selective laser melting test was 316L stainless steel powder with the particle size range of 15–45 μm (Sino-Euro Materials Technologies of Xi'an Co., Ltd., Xi'an, China). The original powder is spherical, as shown in Figure 1, and its chemical composition is shown in Table 1. The powder size and particle size selected for this experiment resulted in better strength and hardness for the material [22].

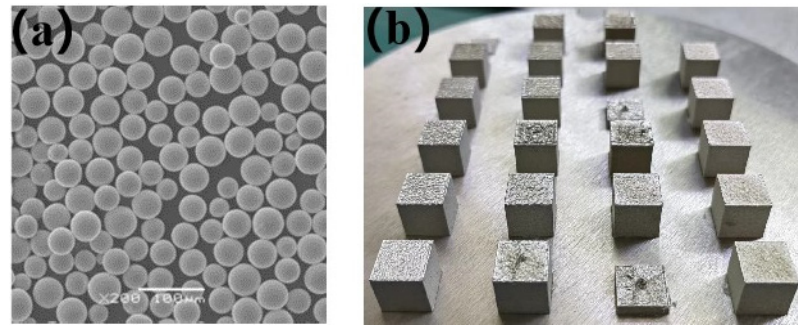


Figure 1. (a) Micograph of the 316L stainless steel powder; (b) SLM formed specimen.

Table 1. Chemical composition of the 316L stainless steel powder (mass fraction %).

Mo	Fe	Cr	Ni	P	S	Cu	C	Si	N	Mn
2.25%–3%	balance	17%–19%	13%–15%	≤0.025%	≤0.01%	≤0.5%	≤0.03%	≤0.1%	≤0.1%	≤2%

The HBD-150 fiber laser (Guangdong Hanbang 3D Tech Co., Ltd., Zhongshan, China) was used in the selective laser melting test equipment. The maximum power of the laser is 200 W. The spot diameter is 65 μm. The molding size of the equipment is φ 159 mm × 100 mm. The specific processing parameters are shown in Table 2. The printing size was 10 × 10 × 10 mm³ cube sample. The protective gas was 99.9% purity argon. The printed sample was processed into 10 mm × 10 mm × 2 mm blocks by wire cutting. The schematic diagram of the SLM process is shown in Figure 2.

Table 2. Processing parameters of laser selective melting test.

Process Parameter	Value
Scanning speed (mm/s)	1000
Laser power (W)	160
Scanning interval (mm)	0.07
Rotation angle (°)	67
Layer thickness (μm)	30

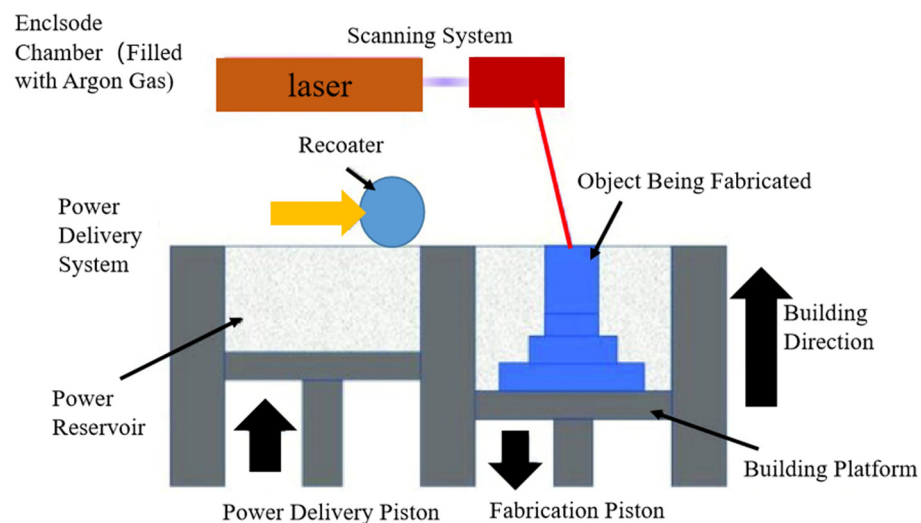


Figure 2. Schematic diagram of SLM process.

A JZ-5020–4DX ultrasonic transducer (Hangzhou Jinyuan Ultrasonic Technology Co., Ltd., Hangzhou, China) was used in the ultrasonic impact test. The amplitude is 10 μm,

3. Results and Discussion

3.1. Metallographic Structure

Figure 4a shows the optical microscope image of the sample before ultrasonic impact and after corrosion near the surface parallel to the construction direction. The cross-section of the sample is like a periodically arranged “fish scale” molten pool, with close overlap between adjacent pools and clear boundaries. This is the result of Marangoni convection formed in the molten pool during the SLM additive process [23]. Figure 4b shows the optical microscope image of the sample etched near the surface parallel to the construction direction after ultrasonic impact. Compared with the sample before ultrasonic shock treatment, the treated sample forms a deformed layer about 100 μm deep near the surface, and the molten pool boundary is no longer clear.

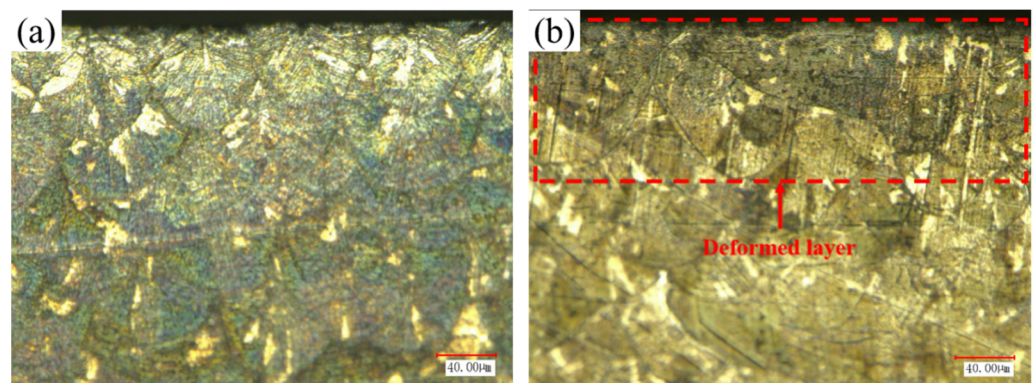


Figure 4. Optical micrograph of near surface microstructure of cross section before and after ultrasonic shock treatment: (a) Untreated sample; (b) Ultrasound impact sample.

3.2. Micro-Hardness

Figure 5 shows the average micro-hardness on the surface and micro-hardness in the depth direction of 316L stainless steel samples by selective laser melting under different treatment methods. It can be seen from the figure that the micro-hardness of samples in the surface and depth direction after ultrasonic impact is higher than that of samples without treatment. It can be seen from Figure 5a that the average surface micro-hardness of 316L stainless steel sample manufactured by selective laser melting after ultrasonic impact is 283.6 HV is about 13.5% higher than that of the untreated 316L stainless steel sample. As shown in Figure 5b, when the surface of the sample is subjected to ultrasonic impact treatment, the surface of the sample is hardened to a certain depth. However, the micro-hardness in the depth direction gradually decreases with the deepening of the depth, and the depth of the affected layer is about 400–500 μm . Then, the micro-hardness component in the depth direction of the sample is close to the hardness of the matrix. Ultrasonic impact has little effect on the micro-hardness at this depth. Therefore, it can be seen that ultrasonic impact can lead to plastic deformation of the material surface and effectively improve the micro-hardness of 316L stainless steel prepared by laser selective melting. At the same time, ultrasonic impact also has a certain strengthening effect on the micro-hardness of 316L stainless steel sample in the depth direction. However, with the deepening of the depth, the effect of the plastic deformation and the work hardening gradually decrease, resulting in a gradual decrease in the depth direction of the hardness.

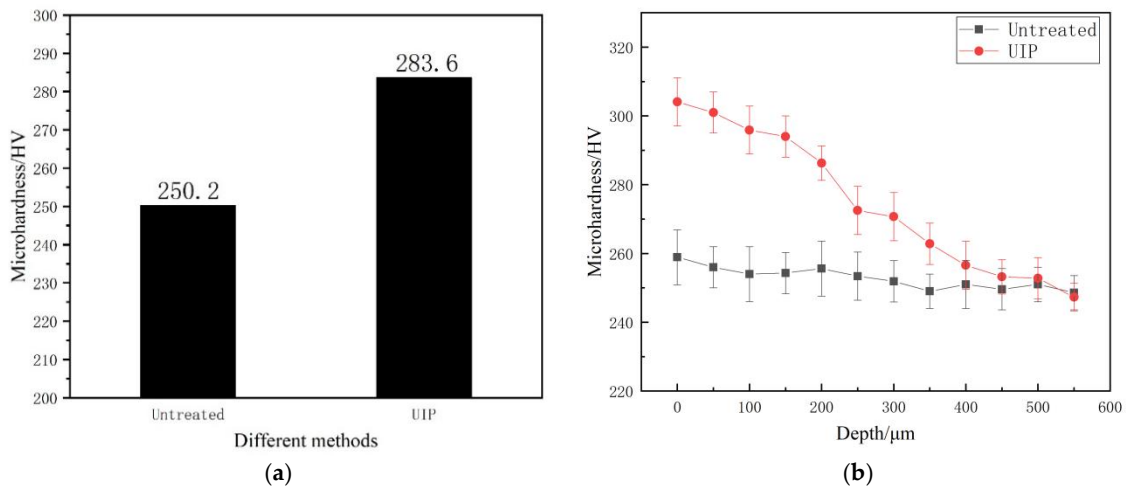


Figure 5. Micro-hardness distribution of samples under different treatment methods: (a) Surface average micro-hardness; (b) Micro-hardness in the depth direction.

3.3. Electrochemical Corrosion

Figure 6 shows the open circuit potential of 316L stainless steel prepared by SLM in the 3.5% NaCl solution before and after the ultrasonic impact. The open-circuit potential reflects the corrosion trend of the sample in the 3.5% NaCl solution. The smaller value of the open circuit potential indicates that the material is more prone to have electrochemical corrosion behavior [24]. As can be seen from Figure 6, after 1200 s the open-circuit potential of 316L stainless steel prepared by SLM after ultrasonic impact gradually tends to be stable, and the maximum open-circuit potential value is 0.01404 V. While the open-circuit potential of 316L stainless steel prepared by SLM without treatment is smaller, floating roughly at -0.1903 V. After the ultrasonic impact, the open circuit potential of the sample is positive, and the open circuit potential of the sample is improved to a certain extent, indicating the possibility of electrochemical corrosion is reduced. The increase of the open circuit potential indicates that the corrosion resistance of the sample has been improved after ultrasonic impact strengthening. This is because the surface hardness of the material has been enhanced under the high-frequency vibration of ultrasonic impact, and the wear resistance of the material has been improved. Therefore, the corrosion resistance of the material has been improved.

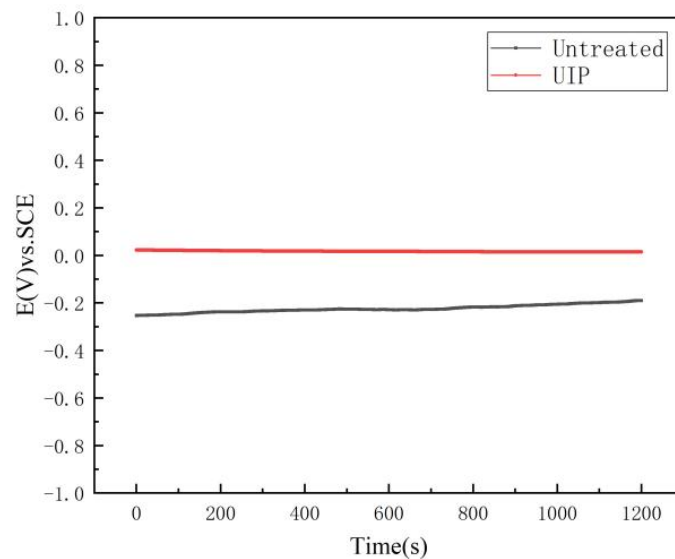


Figure 6. Time-Open Circuit Potential Graph of samples under different treatment methods.

After the open circuit potential reached a certain stable value, the potentiodynamic polarization curves of the 316L samples prepared by SLM in the 3.5% NaCl solution before and after ultrasonic impact were measured, as shown in Figure 7. The curve shown in the figure is obtained after soak in the corrosive solution for 20 min. Compared with the polarization curve of the untreated sample, it is found that the polarization curve shifted to the right after ultrasonic impact strengthening, indicating that the corrosion tendency of the sample decreases. After the ultrasonic shock strengthening, the curve moves slightly downward, indicating that the current density has been decreased to a certain extent and the corrosion performance of the material has been improved. As can be seen from the polarization curve in Figure 7, the self-corrosion potential of the untreated sample is -0.1866 V. After ultrasonic impact strengthening, the self-corrosion potential of the sample is increased to -0.1606 V, moving forward by 250 mV. At the same time, the self-corrosion current density of the untreated samples also decreased from 2.47×10^{-7} to 4.87×10^{-8} $\text{A}\cdot\text{cm}^{-2}$. The higher the self-corrosion potential, the smaller the self-corrosion current density, indicating that the material is less likely to be corroded. Therefore, ultrasonic impact can improve the corrosion resistance of the sample.

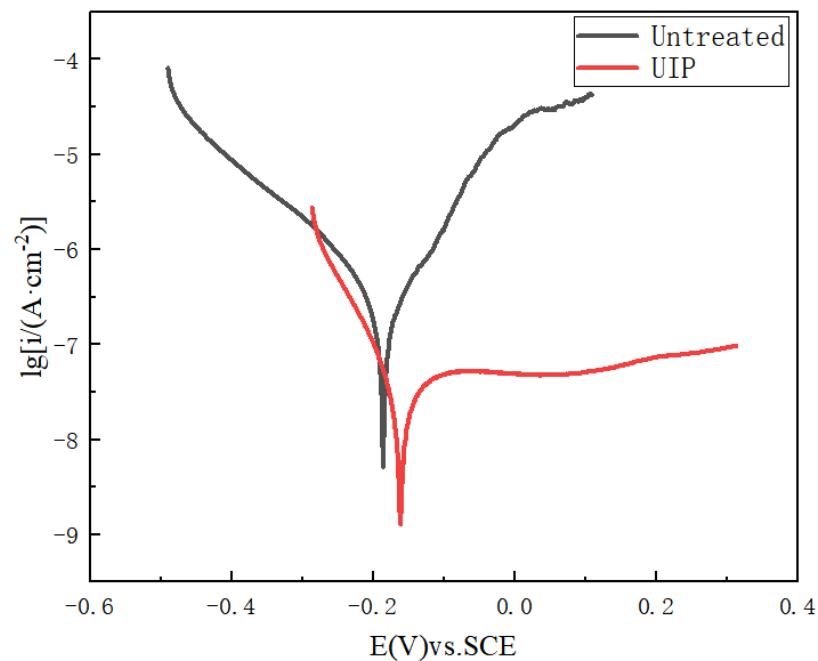


Figure 7. Tafel Curve graph of samples under different treatment methods.

Figure 8 shows the Nyquist curves and bode curves obtained from the electrochemical corrosion test of 316L stainless steel samples prepared by SLM in the 3.5% NaCl solution before and after the ultrasonic impact. It is generally believed that the radius of the impedance circuit is proportional to the impedance of the material. The larger the impedance value, the better the corrosion resistance of the material [25]. It can be found from the Nyquist curve in Figure 8a that plot of the two samples shows a capacitive arc. The impedance arc radius of the untreated sample is relatively small, and the corrosion resistance of the sample is the worst. When the sample is strengthened by the ultrasonic impact on the surface, the impedance arc radius of the sample increases significantly. This shows that the corrosion resistance of the material is improved after the ultrasonic impact. In Figure 8b, it is found that all the phase angles have experienced a process of first increasing and then decreasing. The phase angle of the untreated sample is smaller than that of the ultrasonic impact treated sample. This shows that the corrosion resistance of the sample has been improved after ultrasonic impact.

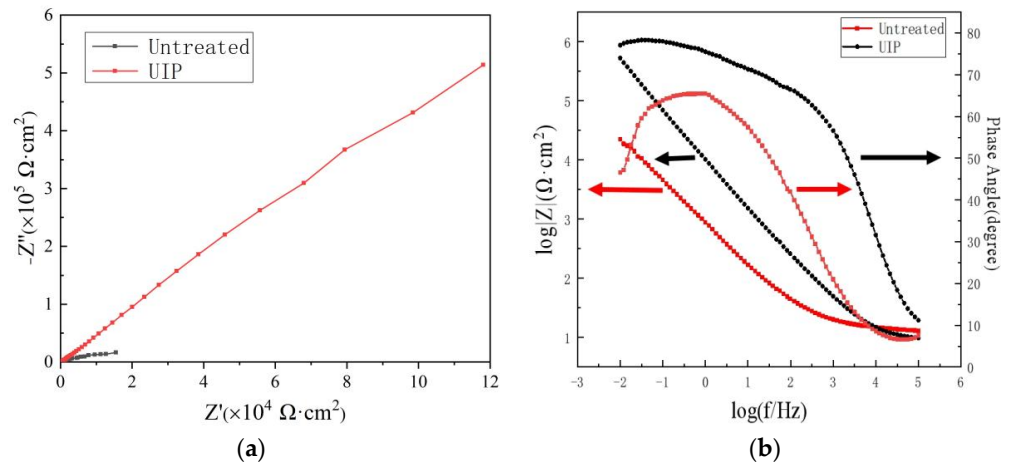


Figure 8. (a) Nyquist Graph (b) Bode Graph.

Figure 9 shows the corrosion morphologies of the untreated sample and the ultrasonic impact sample. It can be seen from Figure 9a that serious corrosion occurs on the surface of the untreated sample, with many corrosion pits and a large area of corrosion on the surface. As can be seen from the partially enlarged Figure 9b, a large number of white corrosion products is produced on the sample surface. It can be seen from Figure 9c that after the ultrasonic impact strengthening, the corrosion area on the surface of the sample becomes smaller. The corrosion pits on the surface also become less and the depth becomes shallower. As can be seen from Figure 9d, the white corrosion production on the surface of the corroded area is also reduced, and the corrosion degree of the surface is also reduced compared with the untreated sample. The material also shows good corrosion resistance. It can be seen that the corrosion resistance of 316L stainless steel prepared by SLM is further improved after ultrasonic impact strengthening.

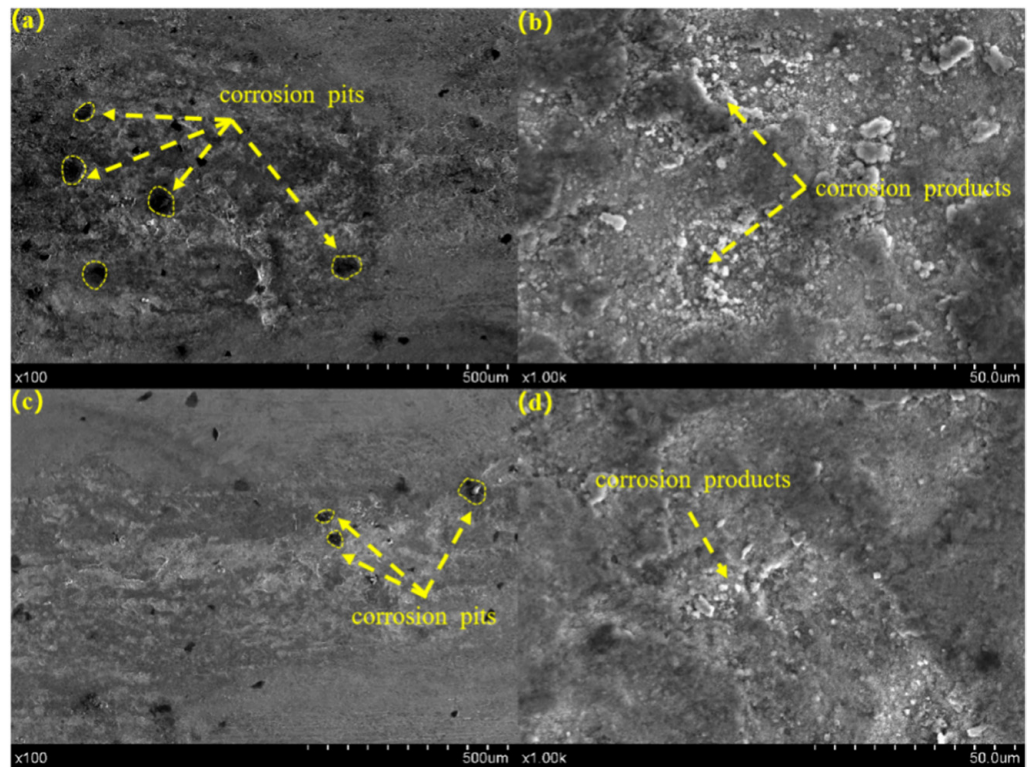


Figure 9. Electrochemical surface corrosion morphology: (a,b) Untreated sample; (c,d) Ultrasonic impact sample.

3.4. Frictional Wear

Due to the low wear resistance of stainless steel itself, the passivation film of stainless steel is often destroyed in the seawater environment, which affects the corrosion performance of stainless steel. Therefore, the wear resistance of stainless steel is an important factor affecting the corrosion resistance. Figure 10 shows the influence of ultrasonic impact on the friction and wear properties of the 316L stainless steel sample. Figure 10a shows the variation curve of the friction coefficient of the sample with different treatment methods. Figure 10b shows the average friction coefficient of the sample before and after ultrasonic impact. It can be seen from Figure 10a that the trend of the friction coefficient curves of the two samples is basically the same. Because the surface of the untreated sample has not been undergone any strengthening treatment. The surface microstructure is relatively loose, and the surface microstructure is easier to peel off when it is worn. However, the surface of the sample after ultrasonic impact is hardened, and the surface hardness is improved. As a result, the friction coefficient of the sample decreases. The average friction coefficient of the samples before and after ultrasonic impact is shown in Figure 10b. Compared with the untreated sample, the surface hardness of the sample after ultrasonic impact increased, and the average friction coefficient decreased by 5.3%.

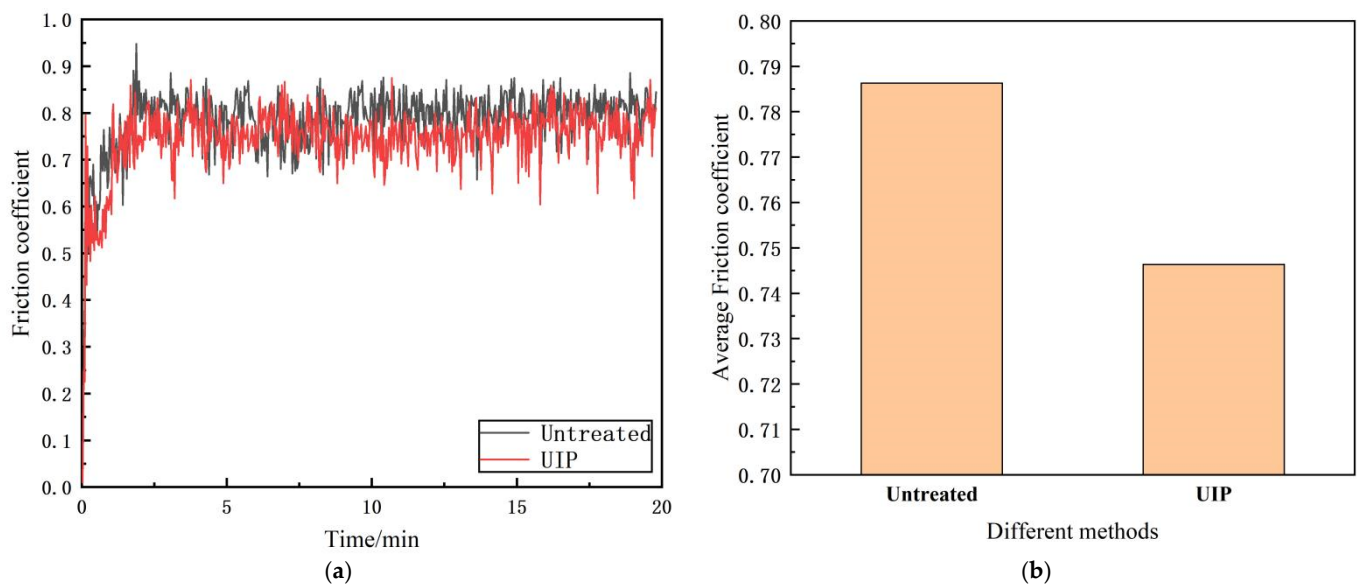


Figure 10. Friction and wear properties of samples under different treatment methods: (a) Friction coefficient-time curve; (b) Average Friction coefficient.

The surface wear morphology of 316L stainless steel samples prepared by SLM before and after ultrasonic impact is shown in Figure 11. Under the friction condition of friction time 20 min and load 2 N, the wear condition of the ultrasonic impact samples is better than that of the untreated samples, and the degree of wear is relatively small. The wear surface of the untreated sample has grooves of wear scars, the shape of the wear marks was complete and clear, and the distribution is uniform. Compared with the untreated sample, the depth of the wear scars of the ultrasonic impact sample is relatively shallow. The distribution of the wear degree on the surface is uneven, and the wear scars are distributed on both sides without obvious cracks. According to the experimental results, the wear resistance of samples after ultrasonic impact is improved, mainly because ultrasonic impact treatment can enhance the microhardness of 316L stainless steel prepared by SLM. Then, it can reduce the friction coefficient of 316L stainless steel, so as to improve the wear resistance and prolong the service life of 316L stainless steel.

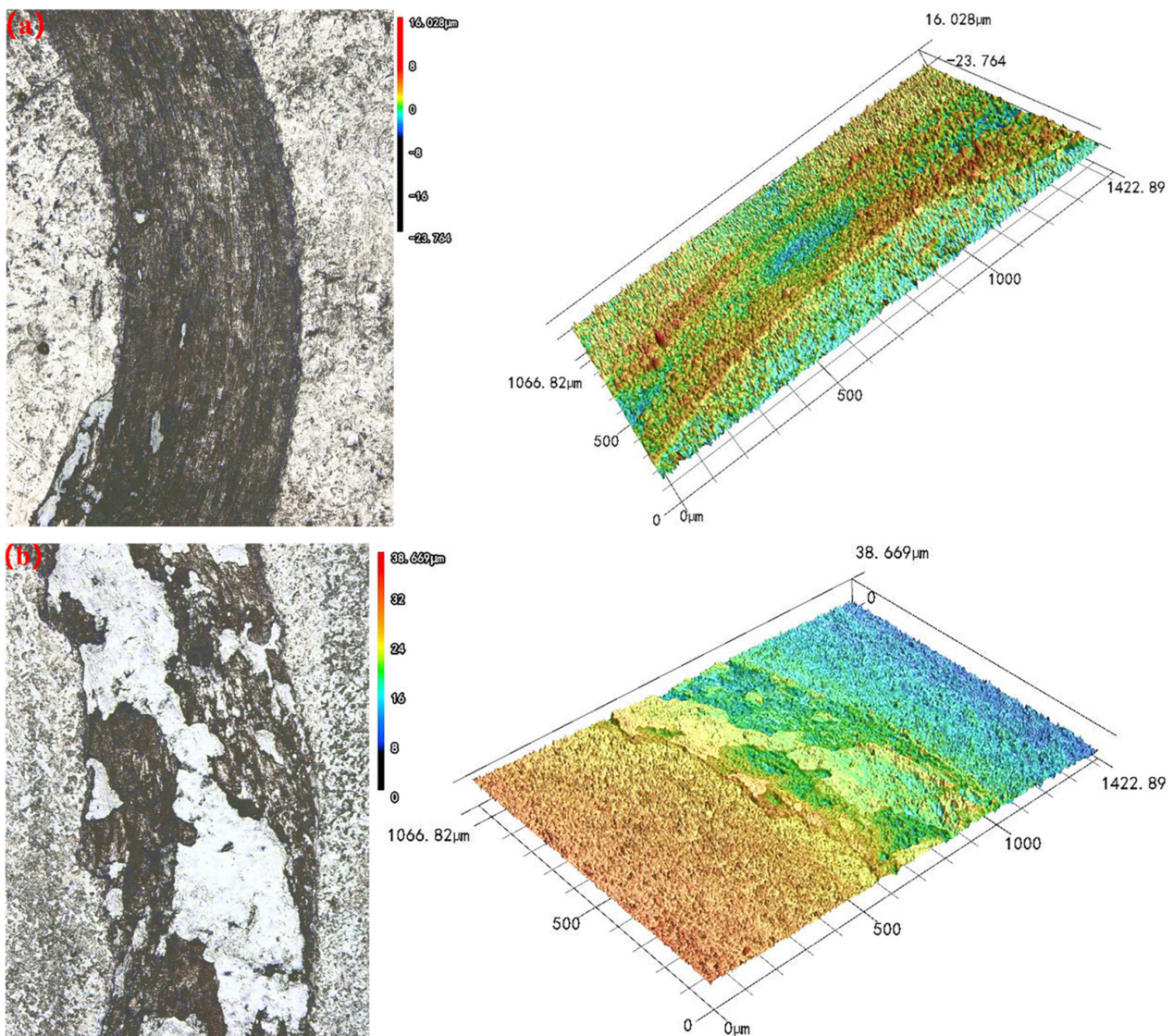


Figure 11. 3D topography of wear scar: (a) Untreated sample; (b) Ultrasonic impact sample.

4. Conclusions

In this paper, an assessment of the ultrasonic impact test of 316L stainless steel prepared by SLM was carried out. The micro-hardness, friction and wear properties, and electrochemical corrosion tests of the untreated sample and the sample after ultrasonic impact were comparatively studied. The main conclusions obtained from the analysis are as follows:

- (1) Ultrasonic impact can significantly improve the surface micro-hardness of 316L stainless steel prepared by SLM. Compared with the untreated sample, the micro-hardness of the sample after ultrasonic treatment is 283.6 HV, which is increased by about 13.5%. Ultrasonic impact can lead to plastic deformation of the material surface, and then improve the micro-hardness of the material.
- (2) According to the results of electrochemical corrosion experiments, the corrosion potential and self-corrosion current density of the samples after ultrasonic impact treatment are slightly higher than those of the untreated samples. The radius of the impedance value arc is larger than that of the untreated samples, indicating that the ultrasonic impact can reduce the corrosion rate of stainless steel surface. It can be seen that ultrasonic impact can improve the corrosion resistance of material.

- (3) Compared with the untreated sample, the friction coefficient of the surface of 316L stainless steel prepared by SLM decreases after ultrasonic impact treatment. The wear scar of the sample after ultrasonic impact treatment is also shallower, so the wear resistance of the 316L stainless steel prepared by SLM after ultrasonic impact is improved.

Author Contributions: Conceptualization and validation, H.C.; writing—original draft preparation and visualization, Z.Z.; resources and methodology, J.Z.; formal analysis, H.J.; supervision, Z.M.; investigation, H.Z.; writing—review and editing, X.M. All authors have read and agreed to the published version of the manuscript.

Funding: This work has been supported by China Postdoctoral Science Foundation projects (NO.2021M691309) and Postdoctoral science foundation projects of Jiangsu Province (NO.2021K245B).

Institutional Review Board Statement: Not applicable.

Informed Consent Statement: Not applicable.

Data Availability Statement: Not applicable.

Acknowledgments: Many thanks to Yizhi Liu for his contribution to funding acquisition and project administration.

Conflicts of Interest: The authors declare no conflict of interest.

References

1. Li, Z.; Yang, Z.; Liu, B.; Yang, S.; Kuai, Z.; Li, J.; Li, H.; Chen, Y.; Wu, H.; Bai, P. Microstructure and mechanical properties of CNC-SLM hybrid manufacturing 316L parts. *J. Manuf. Process.* **2022**, *79*, 432–441. [\[CrossRef\]](#)
2. Chen, J.; Yang, Y.; Song, C.; Zhang, M.; Wu, S.; Wang, D. Interfacial microstructure and mechanical properties of 316L/CuSn10 multi-material bimetallic structure fabricated by selective laser melting. *Mater. Sci. Eng. A* **2019**, *752*, 75–85. [\[CrossRef\]](#)
3. Yu, Z.; Xu, Z.; Guo, Y.; Sha, P.; Liu, R.; Xin, R.; Li, L.; Chen, L.; Wang, X.; Zhang, Z.; et al. Analysis of microstructure, mechanical properties, wear characteristics and corrosion behavior of SLM-NiTi under different process parameters. *J. Manuf. Process.* **2022**, *75*, 637–650. [\[CrossRef\]](#)
4. Xu, R.; Li, R.; Yuan, T.; Niu, P.; Wang, M.; Li, Z. Microstructure, metallurgical defects and hardness of Al–Cu–Mg–Li–Zr alloy additively manufactured by selective laser melting. *J. Alloys Compd.* **2020**, *8*, 35. [\[CrossRef\]](#)
5. Huang, S.; Li, H.; Zhang, H.; Sheng, J.; Agyenim-Boateng, E.; Lu, J. Experimental study and finite element simulation of hydrogen permeation resistance of Ti-6Al-4V alloy strengthened by laser peening. *Surf. Coat. Technol.* **2020**, *400*, 126217. [\[CrossRef\]](#)
6. Liu, B.; Fang, G.; Lei, L. An analytical model for rapid predicting molten pool geometry of selective laser melting (SLM). *Appl. Math. Model.* **2021**, *92*, 505–524. [\[CrossRef\]](#)
7. Du, Z.; Li, H.; Wu, Z.; Yao, L.; Zhao, H. Failure analysis of a ship's seawater pump impeller. *Mater. Prot.* **2019**, *52*, 179–183. (In Chinese)
8. Wang, Q. Application of corrosion and protection technology for seawater circulating pump. *Pet. Petrochem. Mater. Procure.* **2022**, *2*, 69–71. (In Chinese)
9. Varadaraajan, V.; Guduru, R.K.; Mohanty, P.S. Property evolution in amorphous steel coatings by different thermal spray processes. *J. Therm. Spray Technol.* **2022**, *31*, 1056–1066. [\[CrossRef\]](#)
10. Zhang, Q.; Wang, L.; Mei, X.; Yao, J. Research on the development of laser surface modification technology. *China Eng. Sci.* **2020**, *22*, 71–77. (In Chinese) [\[CrossRef\]](#)
11. Nie, L.; Wu, Y.; Gong, H.; Chen, D.; Guo, X. Effect of shot peening on redistribution of residual stress field in friction stir welding of 2219 aluminum alloy. *Materials* **2020**, *13*, 3169. [\[CrossRef\]](#) [\[PubMed\]](#)
12. Li, L.; Kim, M.; Lee, S.; Kim, J.; Kim, H.; Lee, D. Study on surface modification of aluminum 6061 by multiple ultrasonic impact treatments. *Int. J. Adv. Manuf. Technol.* **2018**, *96*, 1255–1264. [\[CrossRef\]](#)
13. Liu, X. Study on Microstructure and properties of 316L stainless steel composites reinforced by laser selective melting particles. *Equip. Manuf. Technol.* **2020**, *2*, 213–215. (In Chinese)
14. Yuan, S.; Wang, D.; Wang, J.; Wang, C.; He, Q.; Cai, X.; Hu, W. Effect of laser surface treatment on corrosion resistance of 316L austenitic stainless steel. *Surf. Technol.* **2021**, *50*, 83–89. (In Chinese)
15. Karimi, M.S.; Yeganeh, M.; Zaree, S.; Eskandari, M. Corrosion behavior of 316L stainless steel manufactured by laser powder bed fusion (L-PBF) in an alkaline solution. *Opt. Laser Technol.* **2021**, *138*, 106918. [\[CrossRef\]](#)
16. Li, L.; Kim, M.; Lee, S.; Kim, T.; Lee, J.; Lee, D. A two-step periodic micro-nano patterning process via ultrasonic impact treatment on a rough SUS301 stainless steel surface. *Surf. Coat. Technol.* **2017**, *330*, 204–210. [\[CrossRef\]](#)
17. Zhang, Q.; Duan, B.; Zhang, Z.; Wang, J.; Si, C. Effect of ultrasonic shot peening on microstructure evolution and corrosion resistance of selective laser melted Ti-6Al-4V alloy. *J. Mater. Res. Technol.* **2021**, *11*, 1090–1099. [\[CrossRef\]](#)

18. Alharbi, N. Shot peening of selective laser-melted SS316L with ultrasonic frequency. *Int. J. Adv. Manuf. Technol.* **2022**, *119*, 2285–2299. [[CrossRef](#)]
19. Eremin, A.V.; Burkov, M.V.; Panin, S.V.; Byakov, A.V. Fatigue crack growth of SLM Ti-4Al-6V processed by ultrasonic impact treatment. *AIP Conf. Proc.* **2019**, *2167*, 20082.
20. Yang, D.; Wang, X.; Peng, Y.; Zhou, Q.; Wang, K. Study on Microstructure and properties of 316L stainless steel fabricated by ultrasonic impact assisted melting electrode arc additive. *Mater. Guide* **2022**, *36*, 126–129. (In Chinese)
21. Yuan, D.; Shao, S.; Guo, C.; Jiang, F.; Wang, J. Grain refining of Ti-6Al-4V alloy fabricated by laser and wire additive manufacturing assisted with ultrasonic vibration. *Ultrason. Sonochem.* **2021**, *73*, 105472. [[CrossRef](#)] [[PubMed](#)]
22. Zeng, F.; Yang, Y.; Qian, G. Fatigue properties and S-N curve estimating of 316L stainless steel prepared by SLM. *Int. J. Fatigue* **2022**, *162*, 106946. [[CrossRef](#)]
23. Yin, Y. *Study on Flow Rule, Microstructure and Properties of 316L Stainless Steel by Selective Laser Melting*; Beijing University of Science and Technology: Beijing, China, 2019. (In Chinese)
24. Chen, L.; Richter, B.; Zhang, X.; Ren, X.; Pfefferkorn, F.E. Modification of surface characteristics and electrochemical corrosion behavior of laser powder bed fused stainless-steel 316L after laser polishing. *Addit. Manuf.* **2019**, *32*, 101013. [[CrossRef](#)]
25. Auezhan, A. Effect of local treatment temperature of ultrasonic nanocrystalline surface modification on tribological behavior and corrosion resistance of stainless steel 316L produced by selective laser melting. *Surf. Coat. Technol.* **2020**, *398*, 126080.